

*Heavy metals in soil of an urban industrial zone in a metropolis: risk assessment and source apportionment*

**Yanyao Li, Yuan Yuan, Chengju Sun,  
Ting Sun, Xianglin Liu, Jianbin Li, Lei  
Fang & Zhengqiu Fan**

**Stochastic Environmental Research  
and Risk Assessment**

ISSN 1436-3240


Stoch Environ Res Risk Assess  
DOI 10.1007/s00477-020-01779-z



**Your article is protected by copyright and all rights are held exclusively by Springer-Verlag GmbH Germany, part of Springer Nature. This e-offprint is for personal use only and shall not be self-archived in electronic repositories. If you wish to self-archive your article, please use the accepted manuscript version for posting on your own website. You may further deposit the accepted manuscript version in any repository, provided it is only made publicly available 12 months after official publication or later and provided acknowledgement is given to the original source of publication and a link is inserted to the published article on Springer's website. The link must be accompanied by the following text: "The final publication is available at [link.springer.com](http://link.springer.com)".**



# Heavy metals in soil of an urban industrial zone in a metropolis: risk assessment and source apportionment

Yanyao Li<sup>1</sup> · Yuan Yuan<sup>1</sup> · Chengju Sun<sup>1</sup> · Ting Sun<sup>1</sup> · Xianglin Liu<sup>1</sup> · Jianbin Li<sup>2</sup> · Lei Fang<sup>1</sup> · Zhengqiu Fan<sup>1</sup> 

© Springer-Verlag GmbH Germany, part of Springer Nature 2020

## Abstract

The risk of heavy metal pollution in industrial zones has received great awareness, but few studies have focused on urban industrial zone of metropolises. In order to explore the pollution characteristic, ecological risks, human health risks, and sources apportionment of heavy metals (HMs), the concentrations of 9 HMs (As, Cd, Cr, Cu, Hg, Mn, Ni, Pb, Zn) in 48 soil sites of a typical urban industrial zone in Shanghai, China were investigated. The mean concentrations of HMs except As (8.09 µg/g) were higher than the background value of corresponding HMs in Shanghai, with Mn (717.60 µg/g) having the highest concentration. The geo-accumulation index showed that Mn had the most severe pollution. The potential ecological risk index indicated that most HMs were at lower risk, but Hg posed a relatively high risk in many sites. In addition, the entire study area may cause potential ecological risks, especially in the northern and the southeastern areas. In light of the results regarding health risk assessment for children and adults, HMs were negligible of non-carcinogenic risk in humans. As for carcinogenic risk, all HMs had “no significant” cancer risk, except for Cr and Ni at the “acceptable” levels. The results of source apportionment analysis using the positive matrix factorization model indicated that heavy metal pollution was mainly caused by (1) metal manufacturing, (2) machinery manufacturing, (3) pesticides and fertilizers, and (4) manufacture and metallic materials. Our results provide the underlying insights needed to guide soil pollution management and remediation of urban industrial areas in metropolises.

**Keywords** Heavy metals · Urban industrial zone · Ecological risk assessment · Source apportionment · Positive matrix factorization

## 1 Introduction

Due to its toxicity, persistence and long-time accumulation, heavy metal (HM) pollution has been a primary soil environmental matter (Zhang et al. 2017; Ren et al. 2019).

Heavy metals (HMs) accumulated in soil will not only cause deterioration of soil environmental quality, but also cause negative effects on human health because humans can absorb HMs through inhalation, dermal absorption and ingestion (Islam et al. 2015; Gao and Wang 2018; Zhang et al. 2018).

**Electronic supplementary material** The online version of this article (<https://doi.org/10.1007/s00477-020-01779-z>) contains supplementary material, which is available to authorized users.

✉ Lei Fang  
fanglei@fudan.edu.cn

✉ Zhengqiu Fan  
zhqfan@fudan.edu.cn

<sup>1</sup> Department of Environmental Science and Engineering, Fudan University, Shanghai 200433, China

<sup>2</sup> Ji'an Institute of Environmental Science, Ji'an 343000, Jiangxi, China

To explore the ecological risk, various technical methods, such as geo-accumulation index, potential ecological risk index, contamination factor, Nemerow pollution index and pollution load index were developed according to the total concentration, bioavailability and toxicity of the HMs, and widely used to evaluate HM pollution in soil (Zhao and Li 2013; Trujillo-Gonzalez et al. 2016; Men et al. 2018; Wu et al. 2018). Most of the previous studies regarding soil HM pollution have been conducted in different sized regions and cities (Gao and Wang 2018; Guan et al. 2018; Zhang et al. 2019), and there are some studies focused on the traditional industrial area, as industrial areas are more

susceptible to HM pollution (Chen et al. 2016; Gao and Wang 2018). In order to cope with the city's economic development, urban industrial zones have gradually emerged in China and have many emerging enterprises with various industrial types. Due to diverse sources of HM pollution and certain large populations, HM pollution in soil of urban industrial zones in metropolis may yet pose greater potential ecological risks and health hazards. However, these impacts and potential risks of HM pollution in the soil of urban industrial zones have not been fully explored.

Understanding the source of HMs in soil is meaningful for the control of HM soil pollution. Source analysis provides a basic analytical tool for preventing and controlling the pollution (Ren et al. 2019). Khademi et al. (2019) used enrichment factor (EF) and found that among the elements studied, Pb, Zn, and Cu were most enriched, especially in street dust in industrial area. Yan et al. (2018) used principal component analysis (PCA) and Pearson correlation analysis to classify the potential sources for each group of trace metals based on their distribution. It was found that most of trace metals in the roadside soil were mainly controlled and influenced by traffic activity. Principal component analysis used with a multiple linear regression (PCA-MLR) is the most widespread model (Yang et al. 2013). Latif et al. (2015) used this method when it was found that the most HMs in the area were dominated by agricultural and biomass burning. But these methods are employed to extract a small number of latent factors for analyzing relationships among the observed variables (Pathak et al. 2015; Liu et al. 2018), and they can only identify a few independent primary components (Yang et al. 2013). The results of these methods are greatly influenced by the quality of dataset. The positive matrix factorization (PMF) shows better general source allocation capabilities (Chen et al. 2013), and can identify sources by multivariate factor analysis (Jiang et al. 2017). Therefore, the PMF model has better advantages than traditional methods, because it can better deal with missing values and can explain the accuracy of the data. The PMF model uses covariance matrices and correlation matrices to simplify the high-dimensional variables and convert them into multiple composite factors (Phillips and Moya 2014), which cannot only ensure non-negative factor distribution and contribution, but can also handle some inaccurate values (Manousakas et al. 2017). Although the PMF model has been widely used for the source identification of atmospheric, water or sediment pollutants (Gholizadeh et al. 2016; Milic et al. 2016), it has rarely been employed to detect soil pollution sources, especially in urban industrial zones.

In this study, we selected Shebei industrial zone in Shanghai as a case study area, which is located in a

metropolis with high population density (of 20 million people) and developed economy. The purposes of this study were (1) to estimate the concentrations of HMs and identify the distribution of HMs in the soil, (2) to evaluate the levels of HM pollution and human health risks in the area, and (3) to quantitatively analyze the sources of HMs by using the PMF model.

## 2 Materials and methods

### 2.1 Study area

Shebei industrial zone (121.18° E, 31.13° N) is a typical urban industrial zone in Shanghai, China (Fig. 1), and its area is about 765.59 hectares. There are various urban land uses in the study area, such as commercial, residential, small farmland and industrial zones. A large residential area is in the vicinity, with a population of approximately 125,000. The major industries are metal smelting and pressing, building materials processing, electronic equipment manufacturing, machine manufacturing, and there are also some emerging industrial activities in smaller scale. The surrounding area near the industrial zone, including the land on both sides of the road, is mainly unused rural land.

### 2.2 Sampling and analysis

144 topsoil samples (0–20 cm) in 48 sites were collected (three sets of parallel samples). Each sample consisted of a mixture of five sub-samples collected from five spots of an area of about 100 m<sup>2</sup>. The sampling sites were selected on the main road soil in this area, and each site measured with a GPS, whereby it could be plotted onto a map. All samples were air dried, cleared of any waste, sieved by a 1 mm nylon sieve. All samples were stored in bottles for concentration determination.

The concentrations of HMs including As, Cd, Cr, Cu, Hg, Mn, Ni, Pb and Zn were determined. According to the previous studies, As was classified as a heavy metal in the field of environmental science (Khademi et al. 2019; Kumar et al. 2019; Sun et al. 2019), because it has similar hazardous properties to heavy metals. This study also considered As as a heavy metal element for analysis. The methods used for the determination of the HMs are listed in Table 1 (Men et al. 2018). Three duplicates were used for quality control for each sample. In this study, quality control was strictly maintained during the experiment. The recoveries of the studied HMs from the standard reference samples were in the range of 94–108%, and the analytical accuracy measured with relative standard deviation was less than 12%. The errors of repeating the samples are

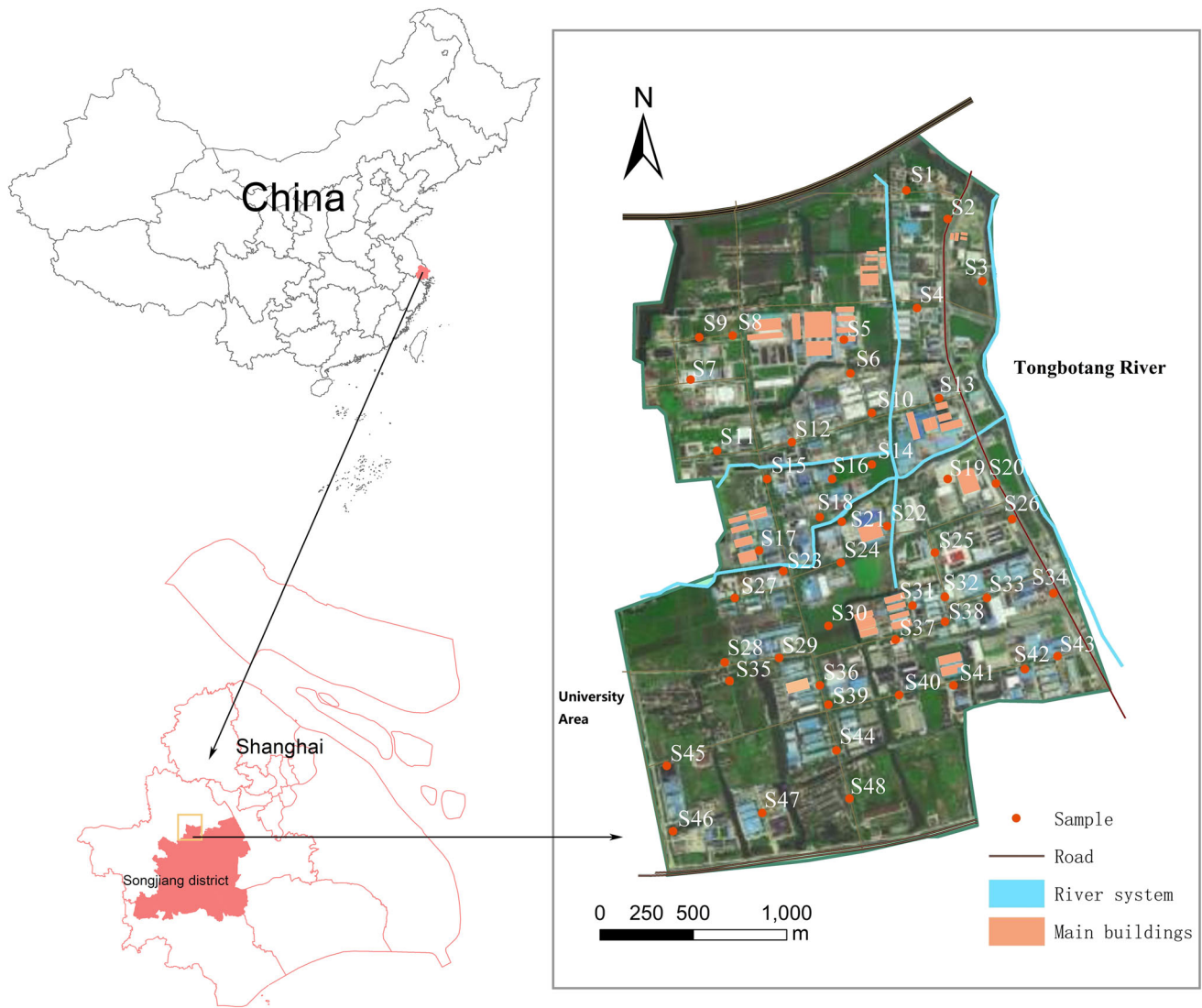


Fig. 1 The study area and sample sites

Table 1 Methods for analyzing HMs

Type of the metal	Type of the method
As	Hydride generation-atomic fluorescence spectrometry (HG-AFS)
Hg	Cold vapor generation-atomic fluorescence detection (CV-AFS)
Cd Cu Ni Pb Zn	Inductively coupled plasma mass spectrometry (ICPMS)
Mn, Cr	Inductively coupled plasma-atomic emission spectrometry (ICP-AES)

within an acceptable range (Table S1). The blank operation method indicated that there was no detectable metal.

### 2.3 Pollution risk assessment method

Geo-accumulation index ( $I_{geo}$ ) is widely applied to assess pollution due to one single element. Meanwhile, for a given factor,  $E_r^i$  means the potential ecological risk factor, and potential ecological risk index (RI) has been used for

pollution assessment in many areas of multiple elements (Awadh 2015).

#### 2.3.1 Geo-accumulation index

The  $I_{geo}$  considers both background values and diagenesis. The formula is (Pathak et al. 2015):

$$I_{geo} = \log_2(C_n/1.5B_n) \tag{1}$$



$C_n$  is the concentration of HM  $n$  of soil and 1.5 is the constant used to neutralize changes caused by diagenesis.  $B_n$  is the geochemical value of background of HM  $n$  (Wang et al. 2009). The different pollution levels of  $I_{geo}$ , which are partitioned in 7 classes according to its value, are listed in Table 2:

### 2.3.2 Potential ecological risk index

The RI can be determined by the following formula (Hakanson 1980):

$$RI = \sum_{i=1}^n E_r^i \tag{2}$$

$$E_r^i = T_r^i \times C_f^i \tag{3}$$

$$C_f^i = C_{0-1}^i / C_n^i \tag{4}$$

$E_r^i$  represents a given substance named the potential ecological risk factor.  $T_r^i$  is a toxic response factor. The  $T_r^i$  for As, Cd, Cr, Cu, Hg, Mn, Ni, Pb, and Zn are 10, 30, 2, 5, 40, 1, 5, 5, and 1, respectively.  $C_f^i$  is a pollution factor,  $C_{0-1}^i$  is the average concentration, and  $C_n^i$  is the geochemical background values of soil. Table 3 shows the values of RI for categorizing the risk level.

### 2.4 Human health risk assessment method

In this study, humans are divided into adults group and children group to determine the potential non-carcinogenic and carcinogenic risks of HMs in surface soil, because their behavior and physiology are different (Taiwo et al. 2016).

Generally, humans are exposed to HM pollution in soil mainly through three ways, including direct ingestion, inhalation, and absorption of soil. The cancer risks (CR) and hazard quotients (HQ) through the three ways mentioned above can be calculated by the following formulas (Ke et al. 2017):

**Table 2** The levels of geo-accumulation index (Muller 1971)

Value	Level
$I_{geo} \leq 0$	Untamated
$0 < I_{geo} \leq 1$	Untamated to moderately contaminated
$1 < I_{geo} \leq 2$	Moderately contaminated
$2 < I_{geo} \leq 3$	Moderately to heavily contaminated
$3 < I_{geo} \leq 4$	Heavily contaminated
$4 < I_{geo} \leq 5$	Heavily to extremely contaminated
$5 < I_{geo}$	Extremely contaminated

**Table 3** The threshold values of RI for determining the ecological risk level (Hakanson 1980)

Value of the RI	Value of the $E_r^i$	Level
$RI \leq 150$	$E_r^i \leq 40$	Low
$150 < RI \leq 300$	$40 < E_r^i \leq 80$	Moderate
$300 < RI \leq 600$	$80 < E_r^i \leq 160$	Considerable
$600 < RI$	$160 < E_r^i \leq 320$	High
	$E_r^i > 320$	Extreme

$$CR_{ingest} = \frac{C_{soil} \times IngR \times EF_e \times ED_e}{BW \times AT} \times CF \times SF \tag{5}$$

$$HQ_{ingest} = \frac{C_{soil} \times IngR \times EF_e \times ED_e}{BW \times AT \times RfD_{ing}} \times CF \tag{6}$$

$$CR_{dermal} = \frac{C_{soil} \times SA \times AF_{soil} \times ABS \times EF_e \times ED_e}{BW \times AT} \times CF \times SF \times GIABS \tag{7}$$

$$HQ_{dermal} = \frac{C_{soil} \times SA \times AF_{soil} \times ABS \times EF_e \times ED_e}{BW \times AT \times RfD_{der}} \times CF \times GIABS \tag{8}$$

$$CR_{inhale} = \frac{C_{soil} \times InhR \times EF_e \times ED_e}{PET \times BW \times AT} \times SF \tag{9}$$

$$HQ_{inhale} = \frac{C_{soil} \times InhR \times EF_e \times ED_e}{PET \times BW \times AT \times RfD_{inh}} \tag{10}$$

$$CR = CR_{ingest} + CR_{dermal} + CR_{inhale} \tag{11}$$

$$HQ = HQ_{ingest} + HQ_{dermal} + HQ_{inhale} \tag{12}$$

where  $CR_{ing}$  and  $HQ_{ing}$  refer to risks through ingestion;  $CR_{der}$  and  $HQ_{der}$  indicate risks through dermal contact;  $CR_{inh}$  and  $HQ_{inh}$  represent risks through inhalation. Details of the parameters used in formula 5–12 were listed in Table S2. The values of  $RfD$  and  $SF$  were listed in Table S3. All the variables and their values refer to the guidelines of US EPA (2016), but some parameters (such as  $BW$ ,  $PEF$ ,  $InhR$  etc.) were adjusted according to the actual situation of China residents in this study.  $HQ$  value stands for Non-carcinogenic risk to the human body. The condition of  $HQ > 1$  indicates the HM pose a non-carcinogenic risk to human; In another condition,  $HQ \leq 1$ , the risk is “insignificant”. In  $HQ$  evaluation, Mn was not analyzed because of the lack of  $RfD_{der}$  and  $RfD_{inh}$ .

$CR$  is the carcinogenic risk due to all pathways. When  $CR > 1 \times 10^{-6}$  and  $\leq 1 \times 10^{-4}$ , it means “acceptable risk”. When  $CR > 1 \times 10^{-4}$ , the risk is

“unacceptable”. If  $CR \leq 1 \times 10^{-6}$ , it represents “no significant” risk. Because of the lack of  $SF$ , this study did not evaluate the risks of Cu, Hg, Mn, Pb, and Zn.

### 2.5 Source identification method

In this study, the PMF model was used to identify the potential sources of HMs from the soil by following the guidelines of the US EPA (2014). The sample concentration data matrix in this model was divided into a factor distribution matrix and a factor contribution matrix. According to the analysis results, the collected overview information and the survey’s emissions inventory, the sources can be defined (Yu et al. 2015). The number of factors was set to 2, 3, 4, 5, and 6, and the number of runs was 40 until the model can be considered stable in this study (Guan et al. 2016). After testing, when the number of factors was 4, the difference between  $Q_{true}$  and  $Q_{robust}$  were minimum and stable, the values of scaled residuals were between -3 and 3, and the signal-to-noise (S/N) ratios of all heavy metals were ranged from 5 to 9 (Table S4).

### 2.6 Statistical analysis

Descriptive statistics of the HMs concentration and health risk assessment performed with Excel Office 2016. The spatial distribution characteristics caused by HMs were represented through the Ordinary Kriging (OK) method in ArcGIS 10.2 software (ESRI, US), and the sample size was sufficient to support robust predictions (Table S5). Origin 2018 (ESRI, US) was used to draw a box plot to determine the data dispersion of  $I_{geo}$  and  $E_r^i$ . Pollution source analysis

was conducted by following the PMF 5.0 (US EPA 2016). The statistical analysis was conducted by using IBM SPSS 22.0 (SPSS, USA).

## 3 Results and discussion

### 3.1 Concentrations of HMs in soil

Generally, the concentrations of HMs in this area were not very high and varies by space and type. As shown in Table 4, the average value of Mn (717.6  $\mu\text{g/g}$ ) was the highest, and the other 8 HMs in the soil could be arranged in decreasing order: Zn (152.67  $\mu\text{g/g}$ ) > Cr (101.64  $\mu\text{g/g}$ ) > Ni (38.52  $\mu\text{g/g}$ ) > Pb (38.29  $\mu\text{g/g}$ ) > Cu (36.66  $\mu\text{g/g}$ ) > As (8.09  $\mu\text{g/g}$ ) > Cd (0.26  $\mu\text{g/g}$ ) > Hg (0.14  $\mu\text{g/g}$ ). The mean concentrations of most HMs, except As, surpassed the corresponding background concentrations, with a value of Zn (152.67  $\mu\text{g/g}$ ) which was twice as high as its background concentration. The mean concentrations of Cu, Cr and Mn were also much higher than their background values.

Shebei industrial zone is a typical urban industrial zone, which is located in a densely populated area. The concentration of most HMs in Shebei industrial zone were much lower than the concentration of the counterparts in BAO steel industry, a traditional industrial area in Shanghai. The average concentration of all HMs except As and Hg in study area were much lower than the concentration of HMs from Shanghai urban street deposited sediments, because this study area was not in the city center, and the traffic was not too heavy. But when compared with

**Table 4** Concentrations of HMs in the study area ( $\mu\text{g/g}$ )

Area	Parameter	As	Cd	Cr	Cu	Hg	Mn	Ni	Pb	Zn	References
Shebei industry zone	Mean	8.09	0.26	101.64	36.66	0.14	717.60	38.52	38.29	152.67	This study
	Media	8.04	0.19	90.05	36.05	0.11	728.00	35.95	31.35	112.00	
	Max	11.40	2.72	391.00	92.00	0.44	980.00	140.00	165.00	918.00	
	Min	6.00	0.12	74.30	20.70	0.03	414.00	24.40	20.00	76.10	
	Variance	1.41	0.14	2196.74	116.30	0.01	13221.20	238.40	563.86	20665.09	
	SD	1.19	0.37	46.87	10.78	0.09	114.98	15.44	23.75	143.75	
	C.V (%)	14.69	141.70	46.11	29.42	63.49	16.02	40.09	62.02	94.16	
Background values of Shanghai	Mean	9.10	0.13	75.00	28.59	0.10	560.20	31.90	25.47	86.10	CNEMC (1990)
BAO steel industry of Shanghai	Mean	0.84	431.40	166.30	34.43	0.23	–	32.85	180.87	202.53	Gao and Wang (2018)
Urban street in Shanghai	Mean	8.01	0.97	264.32	257.63	0.14	–	66.44	236.62	753.27	Shi et al. (2010)
Suburban of Shanghai	Mean	7.70	0.17	–	27.90	0.49	–	–	27.10	131.10	Bi et al. (2018)
The Yangtze River Delta	Mean	9.45	0.20	71.47	27.50	0.12	627.09	30.26	33.91	86.12	Zhou and Wang (2019)

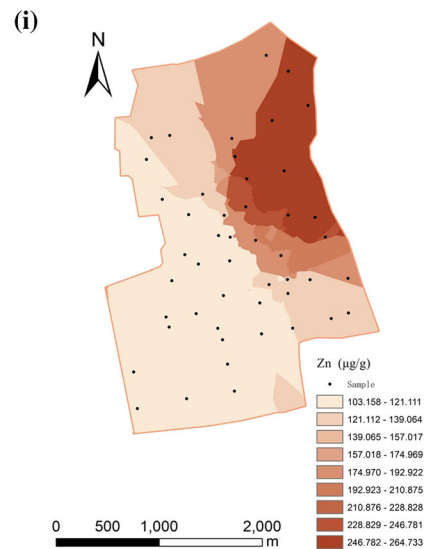
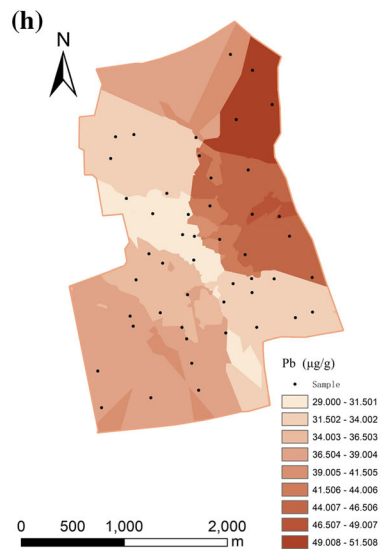
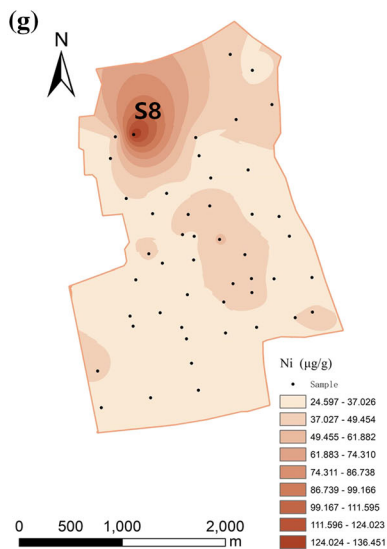
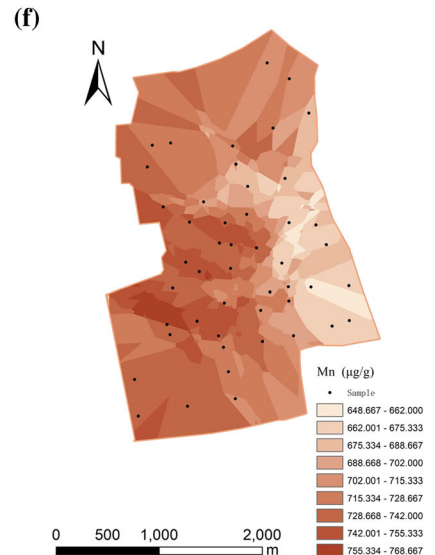
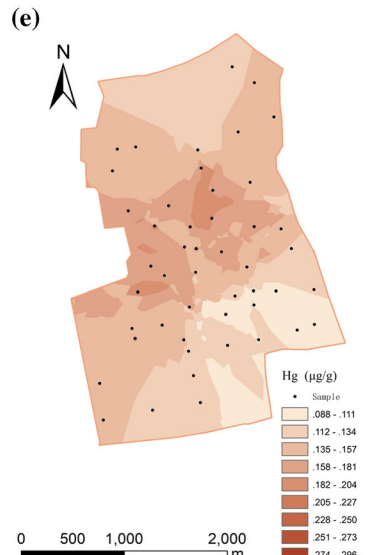
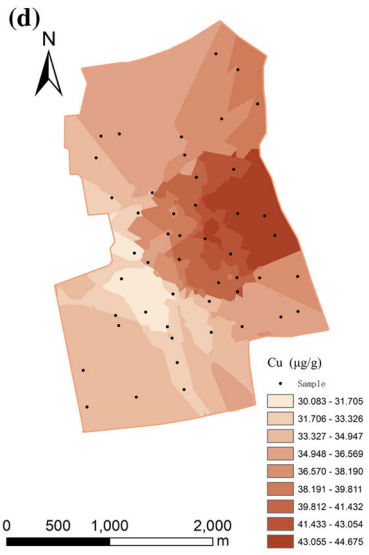
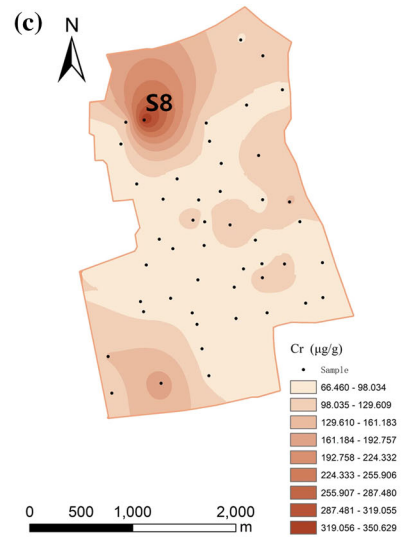
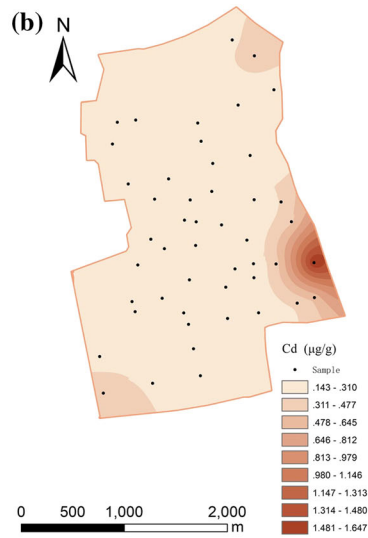
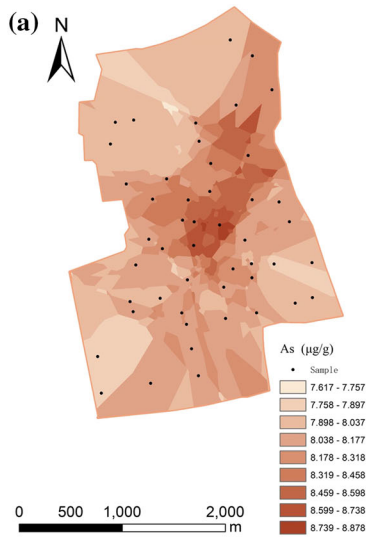




**Fig. 2** The spatial distribution of the concentrations of 9 HMs in the soil of the study area: **a** As, **b** Cd, **c** Cr, **d** Cu, **e** Hg, **f** Mn, **g** Ni, **h** Pb, **i** Zn

suburban areas near various traditional industrial factories in Shanghai, it was obvious that all HM concentrations were higher than the HM concentrations of suburban area except for Hg. The Yangtze River Delta metropolitan cluster centered on Shanghai, however, the concentrations of Mn and Zn of Shebei industrial zone were much higher than the average concentration of that in metropolitan groups. Therefore, Shebei industrial zone was less polluted than the traditional industrial area in Shanghai, but as an emerging urban industrial zone, its HM pollution still needs attention.

The spatial distribution of 9 HM concentrations in the soil of the study area was shown in Fig. 2. For most HMs, except Mn, the higher concentrations were mainly concentrated in the northern and eastern areas. The concentrations of Cr (391  $\mu\text{g/g}$ ) and Ni (140  $\mu\text{g/g}$ ) at the S8 site were at peak levels. This may due to the types of industrial factories surrounding the S8 site, which are mainly lighting appliances and hardware. Cu was also a main heavy metal pollutant with higher concentration in the central and eastern parts, which have some machinery, metal processing and other industries. Mn was highly concentrated in the southwestern part of the study area, which may negatively influence the health of the residents nearby. The high concentration areas of Pb and Zn were mainly located in the eastern part of the area probably due to the color steel factory and building materials factory.

### 3.2 Pollution risks of HMs in soil

Based on the results of  $I_{geo}$ , there is no sampling site polluted by As (Fig. 3a), and most of the sampling sites were

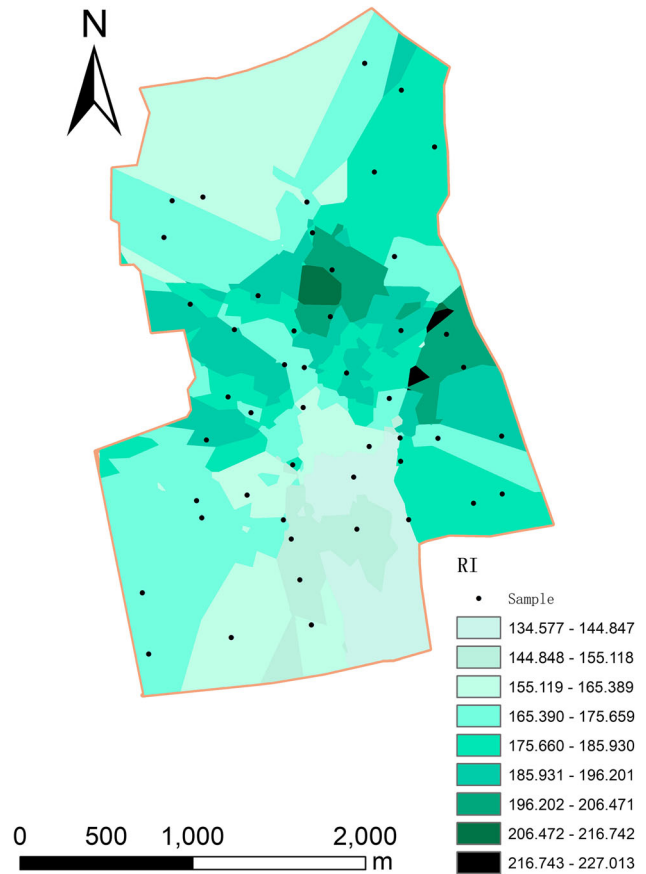


**Fig. 4** Spatial distribution of RI of the HMs in the soil of the study area

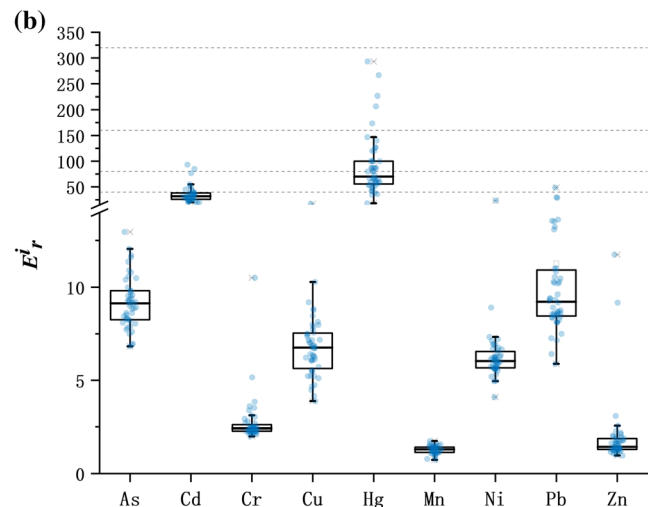
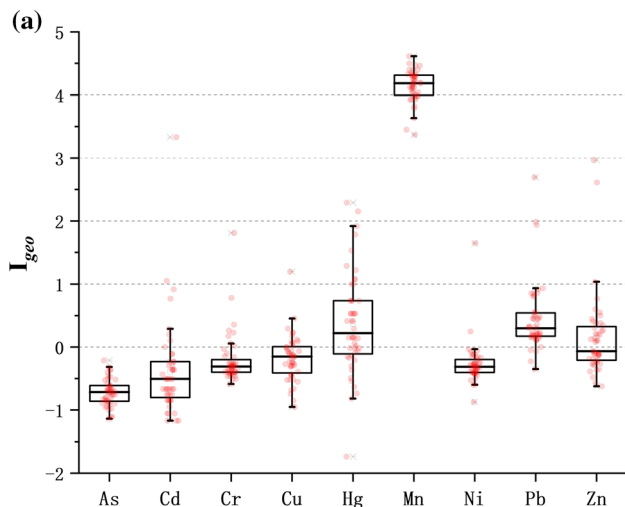


**Fig. 3** Risk assessment results of 9 HMs of study area: **a** the results of the levels of  $I_{geo}$ , **b** the levels of  $E_r^i$  with regards to potential ecological risks

**Table 5** The results of health risk assessment

HM	Group	Non-carcinogenic risks				Carcinogenic risks			
		HQ <sub>ing</sub>	HQ <sub>dermal</sub>	HQ <sub>inh</sub>	HQ	CR <sub>ing</sub>	CR <sub>dermal</sub>	CR <sub>inh</sub>	CR
As	Adult	2.13E-03	4.52E-08	6.52E-06	2.36E-03	1.06E-06	2.04E-11	1.21E-08	1.07E-06
	Children	2.20E-03	4.44E-08	4.43E-06	2.44E-03	1.10E-06	2.00E-11	8.23E-09	1.11E-06
Cd	Adult	2.28E-05	1.80E-08	2.59E-06	2.54E-05	2.28E-08	1.8E-13	1.63E-10	2.30E-08
	Children	2.36E-05	1.76E-08	1.76E-06	2.54E-05	2.36E-08	1.76E-13	1.11E-10	2.37E-08
Cr	Adult	2.96E-03	1.16E-06	3.52E-04	3.32E-03	8.89E-06	6.99E-11	4.23E-07	9.31E-06
	Children	3.06E-03	1.14E-06	2.40E-04	3.31E-03	9.19E-06	6.87E-11	2.88E-07	9.48E-06
Cu	Adult	8.01E-05	2.10E-09	9.04E-08	8.02E-05	–	–	–	–
	Children	8.29E-05	2.06E-09	6.15E-08	8.30E-05	–	–	–	–
Hg	Adult	3.97E-05	4.46E-09	1.58E-07	3.99E-05	–	–	–	–
	Children	4.11E-05	4.38E-09	1.07E-07	4.12E-05	–	–	–	–
Mn	Adult	–	–	–	–	–	–	–	–
	Children	–	–	–	–	–	–	–	–
Ni	Adult	1.68E-04	4.90E-09	1.85E-07	1.69E-04	3.37E-06	2.65E-11	3.21E-09	3.37E-06
	Children	1.74E-04	4.82E-09	1.26E-07	1.74E-04	3.48E-06	2.60E-11	2.18E-09	3.49E-06
Pb	Adult	9.56E-04	5.01E-08	1.08E-06	9.57E-04	–	–	–	–
	Children	9.90E-04	4.93E-08	7.33E-07	9.90E-04	–	–	–	–
Zn	Adult	4.45E-05	1.75E-09	5.05E-08	4.45E-05	–	–	–	–
	Children	4.60E-05	1.72E-09	3.43E-08	4.61E-05	–	–	–	–

not contaminated by Cd, Cr, Cu and Ni. The contamination level of Mn was much higher than any of the other HMs, with its  $I_{geo}$  value higher than 4, indicating “heavily contamination”. Pb and Zn also had “heavy contamination” at some sites.

With regards to potential ecological risks, the  $E_r^i$  value of most HMs except Cd and Hg were lower than 40 at all sampling sites, indicating “low risk” (Fig. 3b). The  $E_r^i$  value of Cd exceeded 40 in some sites, indicating “considerable risk”. However, the  $E_r^i$  of Hg exceeded 40 in all sites, even the values of Hg at some sites were higher than 160, which means at the level of “high risk”. Particularly, there was a site (S21) with an outlier of Hg (293.33), indicating that it was close to “extreme risk”. This site may be related to the proximity of the sampling site to the mechanical processing factories.

Comparing the assessment results of  $E_r^i$  with  $I_{geo}$ , Mn was assessed as a heavy contaminant with  $I_{geo}$ , whereas showing a low risk with  $E_r^i$ . Hg was considered as a moderate contaminant, indicated moderate to high risks. Among the results,  $E_r^i$  and  $I_{geo}$  of Cd at some sites were both higher.

The areas with high RI values were mainly centralized in the north and the southeast (Fig. 4). The risk was lower with decreasing distance to the southwest. Most values of RI across the zone were < 150, indicating a “low risk”; while some values were at the range of 150–300, which

means “considerable risk”. More specifically, some sites in the east suffered “moderate risks” with the values exceeding 300. The heavy metal composites of these sites were superimposed, because there are many types of factories around. Fuel combustion and much of sewage in factories contain large amounts of heavy metal elements (Taylor et al. 2010; Bergthorson et al. 2017). Perhaps the discharge of HMs from factories is the most important factor affecting the concentration of HMs in the soil.

### 3.3 Human health risks posed by HMs in soil

By following the Exposure Factors Handbook (US EPA 2016), hazard quotients (HQ) and carcinogenic risk (CR) of human health can be estimated. With regards to both children and adults, the values of HQ and CR followed the order: ingestion > inhalation > dermal (Table 5). The contribution through ingestion to HQ was little higher than CR. None of the HQ values of HMs > 1, indicating that the non-carcinogenic risk of all HMs was insignificant. For children and adults, Cr and Ni had an “acceptable” cancer risks with CR values ranging from  $1 \times 10^{-6}$  to  $1 \times 10^{-4}$ . Although these two HMs did not show a high ecological risk, they should also be assessed on the aspect of human health risk. Compared with adults, children have a lower risk through ingestion contact and a higher risk through inhalation and dermal contact. The higher risks of

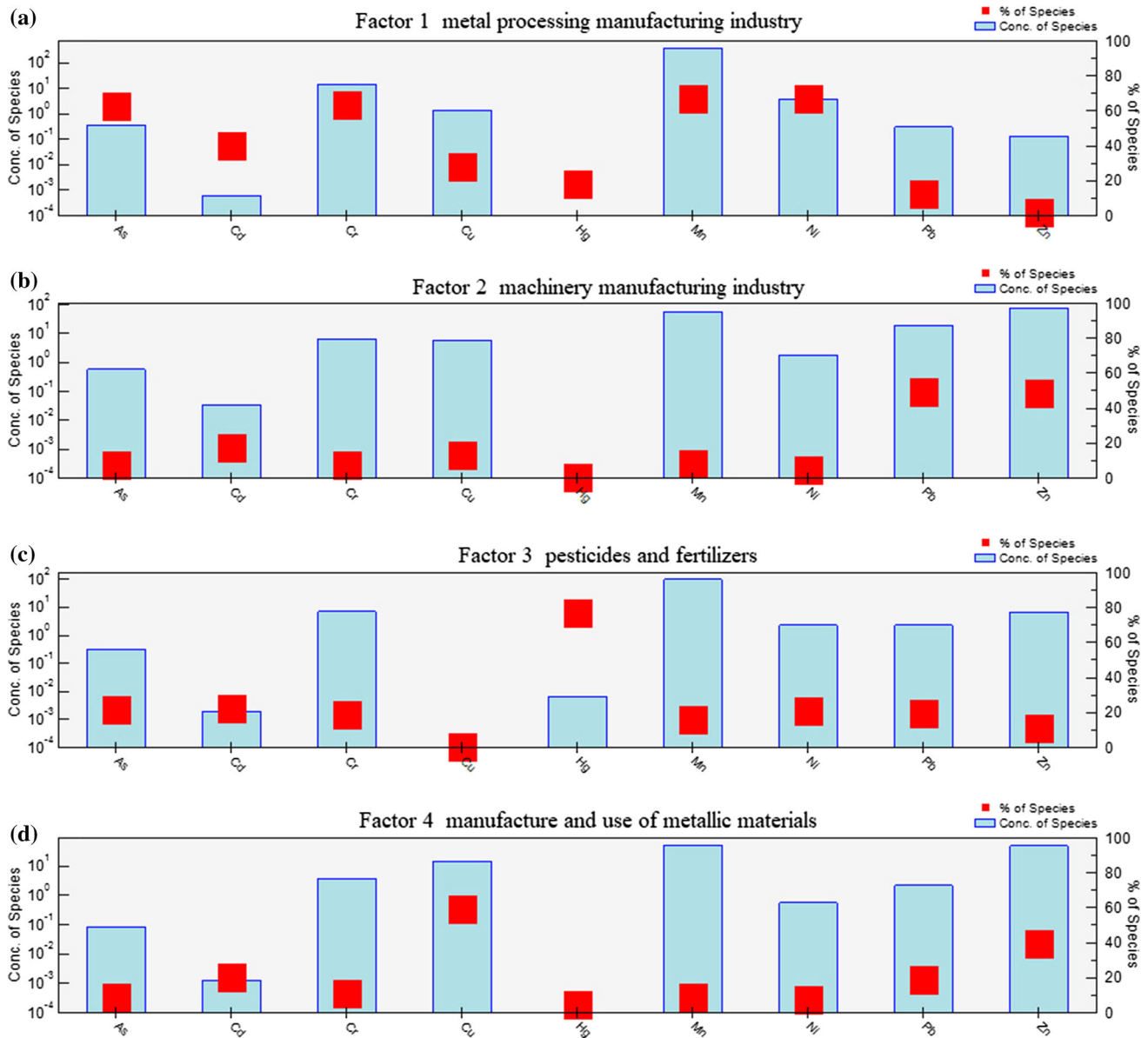


Fig. 5 Factor profile and concentration percentage of HMs in the soil from the PMF model

inhalation and dermal of adults were likely to be caused by the longer duration of exposure (Li et al. 2017). Therefore, although the non-carcinogenic risks caused by the soil HMs were not significant, full attention should be paid to the carcinogenic risks. In addition, there were also many residential areas near the industrial zone, and children should be paid special attention to health risks posed by HMs from the soil.

### 3.4 Quantitative source analysis by using the PMF model

In order to identify quantitatively the source of the soil HMs in the study area, the PMF model was used to analyze

the data by using EPA PMF 5.0 (US) software. The modeling results showed that there were four factors mainly affecting the accumulation and concentration of the 9 HMs (Fig. 5). The contribution of the different elements to each factor was shown in detail in the factor fingerprint (Fig. 6).

In Factor I, As, Cr, Mn and Ni provided 68.3%, 68.6%, 73.2% and 73.0% contribution, respectively. The percentage of Cd was 40.8%, which was also considerable. All these HMs are often used as alloy additives and catalysts, as well as some electroplated materials. Numerous studies demonstrated that Cr, Mn, Ni and Cd usually came from several industrial activities, such as long-term mining, smelting of ores, coal consumption, steel production, and metal processing (Zheng et al. 2010; Li et al. 2011; Qu

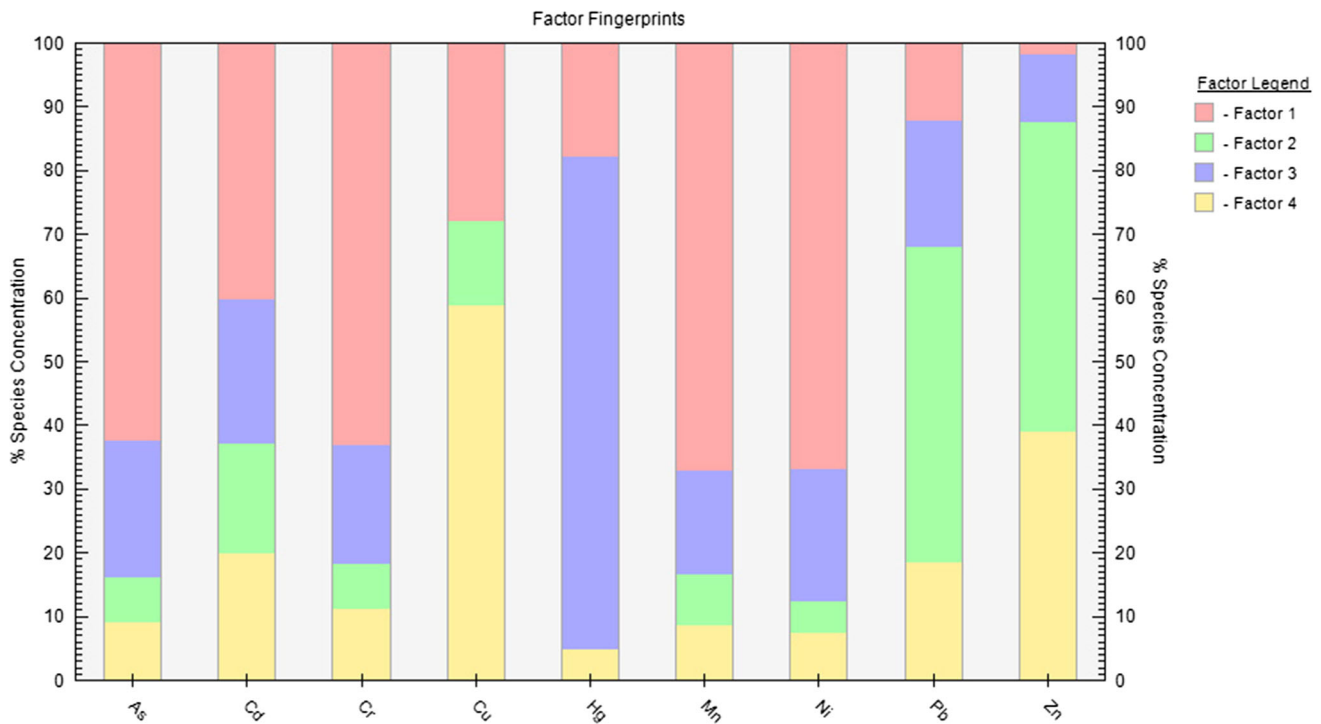


**Fig. 6** Factor fingerprint of 9 HMs based on species concentration (%)

et al. 2013; Yang et al. 2018). There were some metal materials processing plants and automation equipment companies in this area with high concentrations of As, Cr, Mn, Ni and Cd nearby. Therefore, Factor I represents the metal processing manufacturing industry.

Factor II accounted for 54.0% and 52.9% of the concentration of Pb and Zn. Some previously study reported that Pb and Zn in the soil with high concentrations could pose a threat to human health and ecosystems (Dao et al. 2013). Pb, a main element of vehicle emission (Cai et al. 2019), is also widely used in the production of lead storage batteries. Zn might come from vehicle tires (Li et al. 2011), and was widely used in the galvanizing industry due to its excellent corrosion resistance and good mechanical properties. In the automotive and machinery industries, Zn is also used to make batteries. According to the distribution of concentration of these elements, they were concentrated in a manufacturing processing area. Therefore, Factor II may represent the machinery manufacturing industry.

Factor III was significantly affected by the concentration of Hg (70.6%), with other HMs contributed less. According to the results of  $I_{geo}$  and  $E_r^i$  of Hg, most of the sites were polluted which leads to high potential risks. Moreover, the concentration distribution of Hg is relatively uniform. Therefore, a wide range of human activities may be the main sources of Hg, instead of natural sources. Hg is an important element in the composition of pesticides or fertilizers (Guo et al. 2015), which is volatile and easy to

migrate. In spite of little farmland in the study area, long-term use of pesticides and fertilizers in large areas of green land in the study area may also cause Hg pollution. Thus, Factor III may represent the pesticides and fertilizers.

Factor IV was dominated by Cu of 63.9%. Cu is released in the metal processing and smelting industry (Zhang et al. 2004), and being used in the processing of building materials. These activities can discharge a large amount of sewage and dust containing HMs, especially Cu, which will cause pollution to the soil. According to the spatial distribution of Cu, the high concentration sites were located in the eastern part of the study area, where there was a mechanical processing plant. Therefore, Factor IV may be the manufacture and use of metallic materials.

Combining professional knowledge with mathematical models to analyze pollution sources is a common practice in the field of environmental pollution (Guan et al. 2018; Men et al. 2018). Although the PMF model cannot only ensure non-negative factor distribution and contribution, but also handle some inaccurate values, which is more realistic than solutions from general multivariate statistical methods (Chen et al. 2013), the applicability and accuracy of the PMF model in the soil HMs analysis need to be further explored.

## 4 Conclusions

In conclusion, we investigated the pollution characteristics, ecological risks and source apportionment of HMs in the urban industrial area of Shebei industrial zone in Shanghai, China. The mean concentrations of most HMs except As were higher than the background values, with Mn being the highest concentration, and the high concentration values of different HMs had different spatial distribution areas. Geo-accumulation index indicated that the risk levels ranged from “no pollution” (As, Cd, Cr, Ni) to “heavily contaminated” (Mn). According to RI analysis, the potential ecological risks of HMs in the study area were serious, especially in the north and southeast. On the basis of health risk assessment, the contribution of risks through ingestion to HQ was little higher than that to CR. There was insignificant non-carcinogenic risk to either children or adults. The analysis results of the PMF model indicated that four main factors affecting the accumulation of HMs, including (1) metal manufacturing industry, (2) machinery manufacturing industry, (3) pesticides and fertilizers, (4) manufacture and use of metallic materials. Urban industrial zones in metropolis can be closely related to human's health and economic sustainability, and this study can help decision makers to develop more effective exposure reduction and management measures for soil pollution.

**Acknowledgements** This work was supported by the Shanghai Pujiang Program, the National Key Research and Development Program of China (No. 2016YFC0502705).

## References

- Awadh SM (2015) Cd, Ni, and Pb distribution and pollution assessment in roadside dust from Baghdad City and Western Iraqi Desert. *Arab J Geosci* 8:315–323
- Bergthorson JM, Goroshin S, Soo MJ, Julien P, Palecka J, Frost DL, Jarvis DJ (2017) Direct combustion of recyclable metal fuels for zero-carbon heat and power. *Appl Energy* 202:784
- Bi C, Zhou Y, Chen Z, Jia J, Bao X (2018) Heavy metals and lead isotopes in soils, road dust and leafy vegetables and health risks via vegetable consumption in the industrial areas of Shanghai, China. *Sci Total Environ* 619–620:1349–1357
- Cai LM, Wang QS, Wen HH, Luo J, Wang S (2019) Heavy metals in agricultural soils from a typical township in Guangdong Province, China: occurrences and spatial distribution. *Ecotox Environ Safe* 168:184–191
- Chen H, Teng Y, Wang J, Song L, Zuo R (2013) Source apportionment of trace element pollution in surface sediments using positive matrix factorization combined support vector machines: application to the Jinjiang River, China. *Biol Trace Elem Res* 151:462–470
- Chen HY, Teng YG, Lu SJ, Wang YY, Wu J, Wang JS (2016) Source apportionment and health risk assessment of trace metals in surface soils of Beijing metropolitan, China. *Chemosphere* 144:1002–1011
- CNEMC(China National Environmental Monitoring Center) (1990) The background values of chinese soil. Environmental Science Press of China, Hangzhou
- Dao LG, Morrison L, Kiely G, Zhang CS (2013) Spatial distribution of potentially bioavailable metals in surface soils of a contaminated sports ground in Galway, Ireland. *Environ Geochem Hlth* 35:227–238
- Gao J, Wang L (2018) Ecological and human health risk assessments in the context of soil heavy metal pollution in a typical industrial area of Shanghai, China. *Environ Sci Pollut Res Int* 25:27090–27105
- Gholizadeh MH, Melesse A, Reddi L (2016) Water quality assessment and apportionment of pollution sources using APCS-MLR and PMF receptor modeling techniques in three major rivers of South Florida. *Sci Total Environ* 566:1552–1567
- Guan QY, Wang L, Wang FF, Pan B, Song N, Li FC, Lu M (2016) Phosphorus in the catchment of high sediment load river: a case of the Yellow River, China. *Sci Total Environ* 572:660–670
- Guan Q et al (2018) Source apportionment of heavy metals in agricultural soil based on PMF: a case study in Hexi Corridor, northwest China. *Chemosphere* 193:189–197
- Guo W, Huo SL, Ding WJ (2015) Historical record of human impact in a lake of northern China: magnetic susceptibility, nutrients, heavy metals and OCPs. *Ecol Indic* 57:74–81
- Hakanson L (1980) An ecological risk index for aquatic pollution control. A sedimentological approach. *Water Res* 14:975–1001
- Islam MS, Ahmed MK, Habibullah-Al-Mamun M (2015) Apportionment of heavy metals in soil and vegetables and associated health risks assessment. *Stoch Environ Res Risk A* 30:365–377
- Jiang YX, Chao SH, Liu JW, Yang Y, Chen YJ, Zhang AC, Cao HB (2017) Source apportionment and health risk assessment of heavy metals in soil for a township in Jiangsu Province, China. *Chemosphere* 168:1658–1668
- Ke X, Gui SF, Huang H, Zhang HJ, Wang CY, Guo W (2017) Ecological risk assessment and source identification for heavy metals in surface sediment from the Liaohe River protected area, China. *Chemosphere* 175:473–481
- Khademi H, Gabarron M, Abbaspour A, Martinez-Martinez S, Faz A, Acosta JA (2019) Environmental impact assessment of industrial activities on heavy metals distribution in street dust and soil. *Chemosphere* 217:695–705
- Kumar V et al (2019) Pollution assessment of heavy metals in soils of India and ecological risk assessment: a state-of-the-art. *Chemosphere* 216:449–462
- Latif MT, Ngah SA, Dominick D, Razak IS, Guo XX, Srithawirat T, Mushrifah I (2015) Composition and source apportionment of dust fall around a natural lake. *J Environ Sci China* 33:143–155
- Li XH, Tang ZL, Chu FY, Yang LY (2011) Characteristics of distribution and chemical speciation of heavy metals in environmental mediums around Jinchang mining city, Northwest China. *Environ Earth Sci* 64:1667–1674
- Li HH et al (2017) Pollution characteristics and risk assessment of human exposure to oral bioaccessibility of heavy metals via urban street dusts from different functional areas in Chengdu, China. *Sci Total Environ* 586:1076–1084
- Liu YF et al (2018) Comprehensive risk assessment and source apportionment of heavy metal contamination in the surface sediment of the Yangtze River Anqing section, China. *Environ Earth Sci* 77:493. <https://doi.org/10.1007/s12665-018-7621-1>
- Manousakas M, Papaefthymiou H, Diapouli E, Migliori A, Karydas AG, Bogdanovic-Radovic I, Eleftheriadis K (2017) Assessment of PM2.5 sources and their corresponding level of uncertainty in a coastal urban area using EPA PMF 5.0 enhanced diagnostics. *Sci Total Environ* 574:155–164
- Men C, Liu R, Xu F, Wang Q, Guo L, Shen Z (2018) Pollution characteristics, risk assessment, and source apportionment of



- heavy metals in road dust in Beijing, China. *Sci Total Environ* 612:138–147
- Milic A, Miljevic B, Alroe J, Mallet M, Canonaco F, Prevot ASH, Ristovski ZD (2016) The ambient aerosol characterization during the prescribed bushfire season in Brisbane 2013. *Sci Total Environ* 560:225–232
- Muller G (1971) Schwermetalle in den-sediments des Rheins-Veränderungen seitt. *Umhascn* 79:778–783
- Pathak AK, Kumar R, Kumar P, Yadav S (2015) Sources apportionment and spatio-temporal changes in metal pollution in surface and sub-surface soils of a mixed type industrial area in India. *J Geochem Explor* 159:169–177
- Phillips LJ, Moya J (2014) Exposure factors resources: contrasting EPA's exposure factors handbook with international sources. *J Expo Sci Environ Epidemiol* 24:233–243
- Qu MK, Li WD, Zhang CR, Wang SQ, Yang Y, He LY (2013) Source apportionment of heavy metals in soils using multivariate statistics and geostatistics. *Pedosphere* 23:437–444
- Ren Z, Xiao R, Zhang Z, Lv X, Fei X (2019) Risk assessment and source identification of heavy metals in agricultural soil: a case study in the coastal city of Zhejiang Province, China. *Stoch Environ Res Risk A* 33:2109–2118
- Shi G, Chen Z, Bi C, Li Y, Teng J, Wang L, Xu S (2010) Comprehensive assessment of toxic metals in urban and suburban street deposited sediments (SDSs) in the biggest metropolitan area of China. *Environ Pollut* 158:694–703
- Sun L, Guo D, Liu K, Meng H, Zheng Y, Yuan F, Zhu G (2019) Levels, sources, and spatial distribution of heavy metals in soils from a typical coal industrial city of Tangshan, China. *CATENA* 175:101–109
- Taiwo AM et al (2016) Assessment of health risks associated with road dusts in major traffic hotspots in Abeokuta metropolis, Ogun state, southwestern Nigeria. *Stoch Environ Res Risk A* 31:431–447
- Taylor MP, Mackay AK, Hudson-Edwards KA, Holz E (2010) Soil Cd, Cu, Pb and Zn contaminants around Mount Isa city, Queensland, Australia: potential sources and risks to human health. *Appl Geochem* 25:841–855
- Trujillo-Gonzalez JM, Torres-Mora MA, Keesstra S, Brevik EC, Jimenez-Ballesta R (2016) Heavy metal accumulation related to population density in road dust samples taken from urban sites under different land uses. *Sci Total Environ* 553:636–642
- USEPA (United States Environmental Protection Agency) (2014) EPA positive matrix factorization (PMF) 5.0 Fundamentals and User Guide, EPA/600/R-14/108
- USEPA (U.S. Environmental Protection Agency) (2016) Regional screening levels (RSLs) user's guide. Available on <https://www.epa.gov/expobox/about-exposure-factors-handbook>
- Wang J, Chen ZL, Sun XJ, Shi GT, Xu SY, Wang DQ, Wang L (2009) Quantitative spatial characteristics and environmental risk of toxic heavy metals in urban dusts of Shanghai, China. *Environ Earth Sci* 59:645–654
- Wu J, Lu J, Li L, Min X, Luo Y (2018) Pollution, ecological-health risks, and sources of heavy metals in soil of the northeastern Qinghai–Tibet Plateau. *Chemosphere* 201:234–242
- Yan G et al (2018) Enrichment and sources of trace metals in roadside soils in Shanghai, China: a case study of two urban/rural roads. *Sci Total Environ* 631–632:942–950
- Yang B et al (2013) Source apportionment of polycyclic aromatic hydrocarbons in soils of Huanghuai Plain, China: comparison of three receptor models. *Sci Total Environ* 443:31–39
- Yang Q, Li Z, Lu X, Duan Q, Huang L, Bi J (2018) A review of soil heavy metal pollution from industrial and agricultural regions in China: pollution and risk assessment. *Sci Total Environ* 642:690–700
- Yu WW, Liu RM, Wang JW, Xu F, Shen ZY (2015) Source apportionment of PAHs in surface sediments using positive matrix factorization combined with GIS for the estuarine area of the Yangtze River, China. *Chemosphere* 134:263–271
- Zhang T, Wu AL, Guan L, Qi YH (2004) Simulations of metal Cu in heating process. *Chin J Chem* 22:148–151
- Zhang J, Hua P, Krebs P (2017) Influences of land use and antecedent dry-weather period on pollution level and ecological risk of heavy metals in road-deposited sediment. *Environ Pollut* 228:158–168
- Zhang Y, Chen J, Wang L, Zhao Y, Ou P, Shi W (2018) Establishing a health risk assessment for metal speciation in soil—a case study in an industrial area in China. *Ecotoxicol Environ Saf* 166:488–497
- Zhang WP et al (2019) Characterization and evaluation of heavy metal pollution in soil-wheat system around coal mines in Pingdingshan, China. *Appl Ecol Env Res* 17:5435–5447
- Zhao HT, Li XY (2013) Risk assessment of metals in road-deposited sediment along an urban–rural gradient. *Environ Pollut* 174:297–304
- Zheng N, Liu JH, Wang QC, Liang ZZ (2010) Health risk assessment of heavy metal exposure to street dust in the zinc smelting district, Northeast of China. *Sci Total Environ* 408:726–733
- Zhou XY, Wang XR (2019) Impact of industrial activities on heavy metal contamination in soils in three major urban agglomerations of China. *J Clean Prod* 230:1–10

**Publisher's Note** Springer Nature remains neutral with regard to jurisdictional claims in published maps and institutional affiliations.